

Hierarchical quantum master equation approach to current fluctuations in nonequilibrium charge transport through nanosystems

C. Schinabeck^{1,2} and M. Thoss²

¹*Institute for Theoretical Physics and Interdisciplinary Center for Molecular Materials,
Friedrich-Alexander-Universität Erlangen-Nürnberg,
Staudtstr. 7/B2, D-91058 Erlangen, Germany*

²*Institute of Physics, University of Freiburg, Hermann-Herder-Strasse 3, D-79104 Freiburg, Germany*

(Dated: October 23, 2019)

We present a hierarchical quantum master equation (HQME) approach, which allows the numerically exact evaluation of higher-order current cumulants in the framework of full counting statistics for nonequilibrium charge transport in nanosystems. The novel methodology is exemplarily applied to a model of vibrationally coupled electron transport in a molecular nanojunction. We investigate the influence of cotunneling on avalanche-like transport, in particular in the nonresonant transport regime, where we find that inelastic cotunneling acts as trigger process for resonant avalanches. In this regime, we also demonstrate that the correction to the elastic noise upon opening of the inelastic transport channel is strongly affected by the nonequilibrium excitation of the vibration as well as the polaron shift.

In order to characterize and understand electron transport in nanosystems, not only the average current but also its fluctuations and higher-order cumulants of the distribution of transferred charge, the so-called full counting statistics (FCS) [1–3], are of great interest and can be determined in experiments [4–7]. The higher-order current cumulants provide important information, e.g. the study of the current noise (second cumulant) has allowed the determination of the charge of quasiparticles in a superconductor [8–10] and quantum Hall systems [11, 12] as well as of the number and transparency of transmission channels in nanosystems [13–20].

While the FCS in noninteracting systems is described by the Levitov-Lesovik formula [3, 21], the theoretical evaluation of higher-order cumulants is challenging in interacting systems. To this end, different approximate methods have been applied including master equation [22–33] and nonequilibrium Green’s function approaches [31, 34–46], which are either perturbative in nature or rely on special factorization schemes. Although interesting transport phenomena have been revealed by these approximate methods, a reliable and quantitative analysis, in particular in systems with strong coupling, requires the application of methods, which can be systematically converged, i.e. numerically exact methods. In this context, for example, Cohen and coworkers have computed the FCS of the nonequilibrium Anderson impurity model with a quantum Monte-Carlo method [47].

In this paper, the hierarchical quantum master equation (HQME) approach is extended to the evaluation of the FCS for nonequilibrium charge transport. The HQME approach generalizes perturbative master equation methods by including high-order contributions as well as non-Markovian memory and allows for the systematic convergence of the results [48, 49]. The method (also called hierarchical equation of motion (HEOM) approach) was originally developed by Tanimura and Kubo to study relaxation dynamics [50, 51]. Yan and coworkers have extended it to fermionic charge transport [52, 53].

In this context, they [54–62] as well as Härtle *et al.* [48, 49, 63, 64] have investigated electron-electron interactions. We have recently proposed two formulations to treat electronic-vibrational interaction with the HQME approach [65, 66]. To extend the methodology to the evaluation of current fluctuations within the framework of FCS, a counting field is added to the HQMEs and the approach of Flindt *et al.* [26, 67] is employed in the hierarchical Liouville space [55, 68] to obtain the higher-order current cumulants beyond the average current.

We exemplarily apply the novel theoretical methodology to study current fluctuations in nanosystems with strong coupling to mechanical or vibrational degrees of freedom. This is the case, for example, in single-molecule junctions [17, 69–71] and suspended carbon nanotubes [72–74], where strong electronic-vibrational interaction leads to interesting nonequilibrium transport effects, such as switching [75], negative differential resistance [76–80], enhanced current fluctuations [24, 29, 69, 81], decoherence [82, 83], and local heating or cooling [77, 80, 84–88]. Employing the HQME approach, we investigate the influence of cotunneling on avalanche-like transport, in particular in the nonresonant transport regime. In this regime, we also demonstrate that the sign of the inelastic correction to noise at the opening of the inelastic transport channel is strongly influenced by the nonequilibrium vibrational excitation. To be specific, we adopt in the following the terminology used in the context of charge transport in molecular junctions. It should be noted, though, that the methodology is as well applicable to other nanosystems with strong electronic-vibrational coupling as mentioned above.

We consider a model for vibrationally coupled electron transport described by the Hamiltonian $H = H_S + H_{SB} +$

H_B with ($\hbar = 1$)

$$H_S = \sum_m \epsilon_m d_m^\dagger d_m + \sum_\alpha \Omega_\alpha a_\alpha^\dagger a_\alpha + \sum_{m,\alpha} \lambda_{m\alpha} d_m^\dagger d_m (a_\alpha^\dagger + a_\alpha), \quad (1)$$

$H_{SB} = \sum_{k \in L/R, m} (V_{km} d_m^\dagger c_k + h.c.)$, and $H_B = \sum_{k \in L/R} \epsilon_k c_k^\dagger c_k$. Having performed a system-bath partitioning, the molecular subspace (H_S) is considered as reduced system while the leads form the bath (H_B). The molecule is modeled by a set of electronic levels with energy ϵ_m , which are coupled to vibrational modes with frequencies Ω_α via coupling constants $\lambda_{m\alpha}$ and interact with a continuum of electronic states in the leads ($K = L, R$), described by the spectral density $\Gamma_{K,mm'}(\omega) = 2\pi \sum_{k \in K} V_{km}^* V_{km'} \delta(\omega - \epsilon_k)$.

To obtain the FCS $P_R(t, q)$ in the steady state regime, the number q of electrons is counted, which has been collected in the right lead in the time span $[0, t]$. Based on a two-point projective measurement scheme [89], the characteristic function is given by the Fourier transform with respect to q ,

$$G_R(t, \chi) = \sum_q P_R(t, q) e^{i\chi q} = \text{Tr}_{S+B} \{ \rho_{\text{tot}}(t, \chi) \}, \quad (2)$$

where χ is referred to as the counting field and $\rho_{\text{tot}}(t, \chi)$ denotes the density operator of the overall system dressed by χ . In the long time limit, the time derivative of the cumulants $C_R^r(t) = \partial^r / \partial (i\chi)^r \ln G_R(t, \chi)$ corresponds to the steady state zero-frequency current cumulants, $\langle\langle I_R^r \rangle\rangle = \lim_{t \rightarrow \infty} \frac{\partial}{\partial t} C_R^r(t)$. The first two current cumulants are the average current $\langle I \rangle \equiv \langle\langle I_R^1 \rangle\rangle$ and the zero-frequency current noise $S(\omega = 0) \equiv \langle\langle I_R^2 \rangle\rangle$. The dressed density operator $\rho_{\text{tot}}(t, \chi)$ can be written as [89]

$$\rho_{\text{tot}}(t, \chi) = U_\chi(t, 0) \rho_{\text{tot}}(0) U_{-\chi}^\dagger(t, 0), \quad (3)$$

where $U_\chi(t, 0) = \tilde{T} \exp \left(-i \int_0^t d\tau (H_S + H_{SB, \chi}^I(\tau)) \right)$ denotes the dressed time-ordered propagator in the bath interaction picture with $H_{SB, \chi}^I(t) = e^{iH_B t} H_{SB, \chi} e^{-iH_B t}$. To add the counting field χ to the Hamiltonian, we apply the transformation $H_{SB, \chi}^I(t) = e^{i(\chi/2)N_R} H_{SB}^I(t) e^{-i(\chi/2)N_R}$ [89].

Following the standard derivation of the HQME method [53], the following set of EOMs dressed by the

counting field χ is obtained,

$$\begin{aligned} \frac{\partial}{\partial t} \rho_{j_n \dots j_1}^{(n)}(t; \chi) &= - \left(i\mathcal{L}_S + \sum_{r=1}^n \gamma_{j_r} \right) \rho_{j_n \dots j_1}^{(n)}(t; \chi) \\ &- i \sum_{r=1}^n (-1)^{n-r} \mathcal{C}_{j_r} \rho_{j_n \dots j_{r+1} j_{r-1} \dots j_1}^{(n-1)}(t; \chi) \\ &- i \sum_{K, \sigma, l} (\mathcal{A}_{0, K}^{\bar{\sigma}} + \mathcal{A}_{1, K}^{\bar{\sigma}} e^{-\sigma i \chi \delta_{K, R}}) \rho_{(0, K, \sigma, l) j_n \dots j_1}^{(n+1)}(t; \chi) \\ &+ i \sum_{K, \sigma, l} (\mathcal{A}_{0, K}^{\bar{\sigma}} e^{+\sigma i \chi \delta_{K, R}} + \mathcal{A}_{1, K}^{\bar{\sigma}}) \rho_{(1, K, \sigma, l) j_n \dots j_1}^{(n+1)}(t; \chi), \end{aligned} \quad (4)$$

with

$$\mathcal{C}_{0, K, \sigma, l} \rho^{(n)}(t; \chi) = \eta_l \sum_m V_{K, m} d_m^\sigma \rho^{(n)}(t; \chi), \quad (5a)$$

$$\mathcal{C}_{1, K, \sigma, l} \rho^{(n)}(t; \chi) = (-1)^n \eta_l^* \rho^{(n)}(t; \chi) \sum_m V_{K, m} d_m^\sigma, \quad (5b)$$

$$\mathcal{A}_{0, K}^{\bar{\sigma}} \rho^{(n)}(t; \chi) = \sum_m V_{K, m} d_m^{\bar{\sigma}} \rho^{(n)}(t; \chi), \quad (5c)$$

$$\mathcal{A}_{1, K}^{\bar{\sigma}} \rho^{(n)}(t; \chi) = (-1)^n \rho^{(n)}(t; \chi) \sum_m V_{K, m} d_m^{\bar{\sigma}}. \quad (5d)$$

As the forward and the backward propagator in Eq. (3) carry a different counting-field dependence, the respective contributions are separated in the HQMEs (4) by the index $f = 0, 1$ in the multiindex $j = (f, K, \sigma, l)$. Consequently, the ADOs $\rho_{j_n \dots j_1}^{(n)}(t; \chi)$ fulfill the relation $\sum_{f_n \dots f_1=0,1} \rho_{j_n, \dots, j_1}^{(n)} = \rho_{p_n, \dots, p_1}^{(n)}$, where $\rho_{p_n, \dots, p_1}^{(n)}$ with $p = (K, \sigma, l)$ denote the ADOs of the standard HQME formulation.

The index l originates from the decomposition of the correlation function of the free bath $C_{K, mm'}^\sigma(t) = \langle\langle \check{c}_{K m}^\sigma(t) \check{c}_{K m'}^\sigma(\tau) \rangle\rangle_B$ by a sum over exponentials, i.e. $C_{K, mm'}^\sigma(t) = V_{K m} V_{K m'} \sum_{l=0}^{l_{\max}} \eta_l e^{-\gamma_{K, \sigma, l} t}$, with the bath coupling operators $\check{c}_{K m}^\sigma(t) = e^{iH_B t} (\sum_{k \in K} V_{k m}^\sigma c_k) e^{-iH_B t}$. To this end, the spectral density in the leads is modeled as a single Lorentzian $\Gamma_{K, mm'}(\omega) = 2\pi \frac{V_{K m} V_{K m'} W^2}{(\omega - \mu_K)^2 + W^2}$ and the Fermi distribution is approximated by a sum-over-poles scheme, the so-called Pade decomposition. To mimic the wide-band limit, the band width is chosen as $W = 10^4$ eV.

As the HQMEs (4) are local in time, the recursive scheme proposed by Flindt *et al.* [26, 67], which was originally developed for a lowest-order Markovian ME in the Liouville space of the reduced system, can be employed to evaluate the zero-frequency current cumulants. To this end, the EOMs (4) are represented in matrix-vector form in the hierarchical Liouville space [55, 68], $|\dot{\rho}(t; \chi)\rangle\rangle_H = \mathcal{L}_H(\chi) |\rho(t; \chi)\rangle\rangle_H$ where the column vector $|\rho(t; \chi)\rangle\rangle_H$ contains all ADOs included in the calculation. Following the recursive scheme of Flindt *et al.*, the first two zero-frequency current cumulants are expressed by

$\langle\langle I_R^1 \rangle\rangle = e\langle\langle \tilde{0} | \mathcal{L}_H^{(1)} | 0 \rangle\rangle$ and

$$\langle\langle I_R^2 \rangle\rangle = e^2\langle\langle \tilde{0} | \mathcal{L}_H^{(2)} | 0 \rangle\rangle - 2e^2\langle\langle \tilde{0} | \mathcal{L}_H^{(1)} \mathcal{R} \mathcal{L}_H^{(1)} | 0 \rangle\rangle, \quad (6)$$

where $|0\rangle \equiv |\rho^{\text{st}}\rangle$ and $\langle\langle 0| \equiv \langle\langle \mathbb{1}_S, 0, \dots, 0|$ denote the left and the right eigenvector of $\mathcal{L}_H(\chi = 0)$ with eigenvalue 0, respectively. Additionally, we have defined $\mathcal{L}_H^{(r)} \equiv \partial^r / \partial (i\chi)^r \mathcal{L}_H(\chi)|_{\chi=0}$ and the pseudoinverse $\mathcal{R} = \mathcal{Q} \mathcal{L}_H^{-1} \mathcal{Q}$ with $\mathcal{Q} = 1 - |0\rangle\langle\langle \tilde{0}|$. In case of a noninteracting system ($\lambda_{m\alpha} = 0$), converged results for the current (noise) representing a single-particle (two-particle) observable are obtained by a truncation of the hierarchy at the second (fourth) tier. Cerrillo *et al.* have proposed an alternative HQME method to evaluate the FCS for the case of energy transfer in the spin-boson model where a cascade of hierarchies is set up for the moments of the FCS [90]. This approach could, in principle, be reformulated for fermionic charge transport. However, it cannot be directly solved for the steady state in contrast to our approach outlined above. The frequency-dependent current noise can be calculated following Ref. 91.

In the following, we apply the methodology to study current fluctuations in nanojunctions with strong electronic-vibrational coupling. A particular intriguing nonequilibrium phenomenon in this parameter regime is the existence of avalanche-like transport with giant Fano factors. This was studied previously employing perturbative Markovian rate equations [24, 29]. Here we use the nonperturbative HQME approach to investigate the influence of cotunneling on avalanche-like transport. In order to quantify the noise, the Fano factor is used, which is defined as the ratio between the actual zero-frequency noise and the noise of a Poissonian process, i.e. $F = S(0)/e\langle I \rangle$.

Fig. 1a depicts the Fano factor-voltage characteristics for different energies of the renormalized molecular level, $\tilde{\epsilon}_0 = \epsilon_0 - \lambda^2/\Omega$, and a set of parameters typical for molecular junctions weakly coupled to leads, $\lambda/\Omega = 3$, $\Omega = 0.1$ eV, $T = 100$ K as well as $\Gamma \equiv \Gamma_{L,11} = \Gamma_{R,11} = 10^{-4}$ eV. In the nonresonant transport regime ($\Phi < 2\tilde{\epsilon}_0$), the Fano factor-voltage characteristics obtained by the HQME approach increase with bias voltage until they assume their maximum around $e\Phi \approx 2(\tilde{\epsilon}_0 - \Omega)$. For higher bias voltages, they exhibit a stepwise decrease.

In the resonant transport regime ($\Phi > 2\tilde{\epsilon}_0$), the HQME results are reproduced by Born-Markov (BM) calculations, which neglect higher-order cotunneling effects. In a BM picture, electron transport takes place in resonant avalanches with long waiting times in between. The detailed structure of these avalanches, which start and terminate in the vibrational ground state, has been discussed in Refs. 24 and 29. The corresponding Fano factor is determined by the average number of electrons in a such an avalanche [29, 92]. In contrast, in the nonresonant transport regime, the accurate HQME approach predicts significantly smaller Fano factors compared to the BM method because of the coexistence of resonant avalanches and elastic or inelastic cotunneling (cf. Fig.

2a,b). The latter processes, which lead to Fano factors of the order of one, govern the waiting times [24], which are considerably longer than in the resonant transport regime because both chemical potentials are below the Fermi energy.

For $\tilde{\epsilon}_0 = 0.5$ eV, the Fano factor-voltage characteristics exhibits an oscillatory behavior, which is not captured by the BM approach. While the bias voltages where the Fano factor drops agree with the stepwise decrease in the BM calculation, the bias voltages where this observable increases correspond to peaks in the differential conductance depicted in Fig. 1b. These peaks represent a signature of resonant absorption processes (cf. Fig. 2c) facilitated by the nonequilibrium vibrational excitation induced by inelastic cotunneling. The combination of these processes provides a trigger process for resonant avalanches in the nonresonant transport regime in addition to the sequential process depicted in Fig. 2d, which has to be facilitated by thermal broadening. Figs. 1c and 1d, which depict the Fano factor-voltage characteristics for different lead temperatures T and different molecule-lead coupling strengths Γ , demonstrate that the resonance corresponding to the onset of these trigger processes is shifted to lower bias voltages with increasing lead temperature T and decreasing molecule-lead coupling Γ . This behavior can be rationalized as follows. The resonance requires a significant change in the populations [93, 94], i.e. the probability for deexcitation by

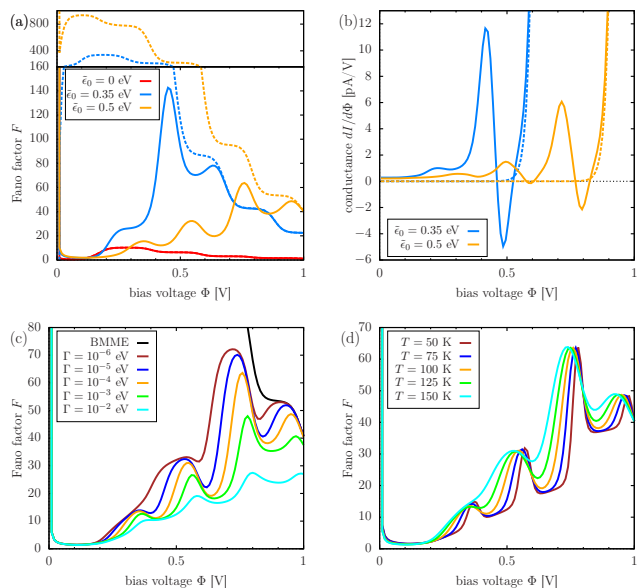


FIG. 1. Fano factor (a,c,d) and conductance (b) as a function of voltage for $\lambda/\Omega = 3$ and $\Omega = 0.1$ eV. In panels a and b, the results are shown for $T = 100$ K, $\Gamma = 10^{-4}$ eV and different energies of the molecular level. In contrast, panel c (d) depicts the Fano factor for $\tilde{\epsilon}_0 = 0.5$ eV and $T = 100$ K ($\Gamma = 10^{-4}$ eV) where the molecule-lead coupling Γ (lead temperature T) is varied. Solid lines represent the numerically exact HQME results while dashed lines show approximate BMME results.

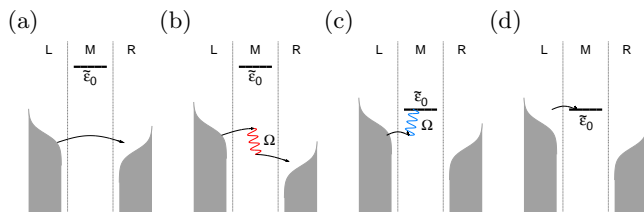


FIG. 2. Illustration of transport processes in the nonresonant transport regime at nonzero temperature of the leads. In panels (a) and (b), an electron tunnels from the left to the right lead via virtual occupation of the molecular bridge. While panel (a) shows an elastic cotunneling process, a similar inelastic cotunneling process is depicted in panel (b) where the vibrational mode is excited by a single vibrational quantum of frequency Ω (red wiggly line). In panels (c) and (d), an electron sequentially tunnels from the left lead onto the molecular bridge, where the process in panel (c) includes the deexcitation of the vibrational mode by a single vibrational quantum and the process in panel (d) is enabled by the thermal broadening of the Fermi distribution.

resonant absorption has to become higher than for excitation by inelastic cotunneling. The different dependence of these processes on temperature and molecule-lead coupling strength explains the observed behavior. A closer inspection of Fig. 1d reveals that the width of the peaks in the Fano factor, that is the distance between the increase and the subsequent decrease of the Fano factor, is proportional to temperature. Consequently, we can conclude that the oscillations are a finite temperature effect, whereas the Fano factor is supposed to exhibit a stepwise increase for zero temperature in the nonresonant transport regime.

Another important aspect of vibrationally-coupled electron transport in nanosystems has been to understand how inelastic effects alter the transport characteristics, in particular close to the threshold bias voltage $e\Phi = \Omega$ [36–39, 41, 95, 96]. In analogy to the current, the onset of inelastic cotunneling at $e\Phi = \Omega$ leads to a negative or positive contribution to the noise, which is reflected by a positive or negative sign of the second derivative of noise with respect to bias voltage. As a representative example, Fig. 3a depicts this observable for parameters $\epsilon_0 = 3 \Omega$, $\lambda/\Omega = 0.6$, $k_B T = 0.0862 \Omega$. Considering the results obtained by a fourth-tier truncation of the HQMEs, we find two transitions: The first one from a positive to a negative contribution between $\Gamma = 2.25 \Omega$ and $\Gamma = 2.5 \Omega$ corresponding to a zero-bias conductance G^{0V} of 0.395 and $0.445 G_0$, respectively (cf. Fig. 3b), where G_0 denotes the conductance quantum. The second crossover from a negative to a positive sign occurs around $\Gamma = 5.5 \Omega$ ($0.8 G_0$). These transitions can be rationalized by the competition between one-electron and coherent two-electron processes, where the former (latter) always gives a positive (negative) contribution to the noise [95].

It is important to emphasize, that the crossover does

not only depend on the zero-bias conductance but, in principle, on all model parameters. This is demonstrated in the color map in Fig. 4, which depicts the inelastic correction to the noise as a function of zero-bias conductance and energy of the molecular level obtained within the HQME approach. To analyze the influence of the nonequilibrium vibrational excitation, the white lines mark the transitions between positive and negative inelastic corrections as obtained by a lowest-order expansion (LOE) in electronic-vibrational coupling, where the full energy dependence of the model is taken into account but the vibration is treated in thermal equilibrium [36]. There are two transition branches $\epsilon_0^{</>LOE}(G^{0V})$ (indicated by solid/dashed white lines). In the limit $\epsilon_0 \gg \Omega$, the crossovers occur at $(1/2 \pm 1/\sqrt{2})G_0$ and thus follow the predictions [36, 37, 95] obtained within the extended wide-band approximation [38, 96]. While there is only one transition from negative to positive sign for $\epsilon_0 = 0.5\Omega$, the inelastic correction is always positive for $\epsilon_0 \leq \Omega/(2\sqrt{2})$. Comparing these LOE results with the two transition branches obtained by the HQME calculations (marked as $\epsilon_0^{</>$ in Fig. 4), we find that the transitions are shifted to $0.46 G_0$ and $0.80 G_0$ for $\epsilon_0 = 3.5 \Omega$. This is a consequence of the nonequilibrium vibrational excitation. In contrast to the upper transition, the lower

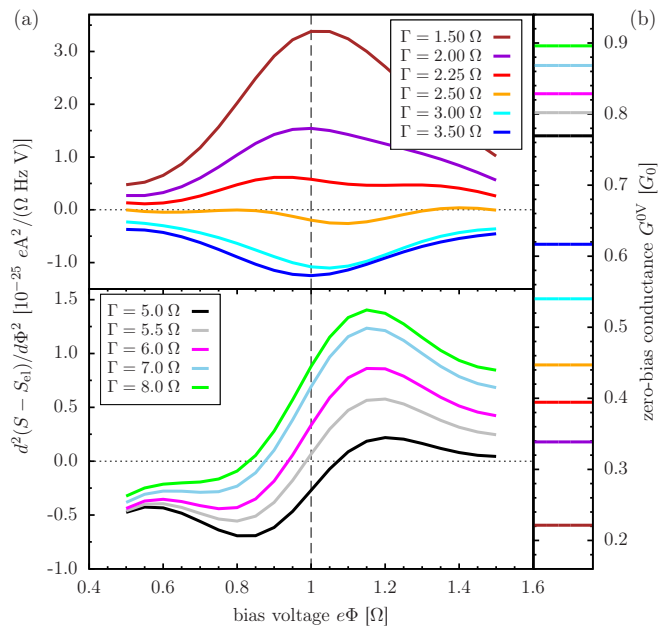


FIG. 3. Inelastic correction to noise (a) measured by the second derivative of the noise with respect to bias voltage for $\epsilon_0 = 3 \Omega$, $\lambda/\Omega = 0.6$, $e\Phi = \Omega$, $k_B T = 0.0862 \Omega$ and different values of the molecule-lead coupling strength Γ . For a better resolution of inelastic effects, the signal S_{el} of a noninteracting single-level model with level energy ϵ_0 is subtracted from the total noise in order to approximately remove the elastic background. The corresponding zero-bias conductance is depicted in panel b. All results have been obtained using a truncation of the hierarchy at the fourth level.

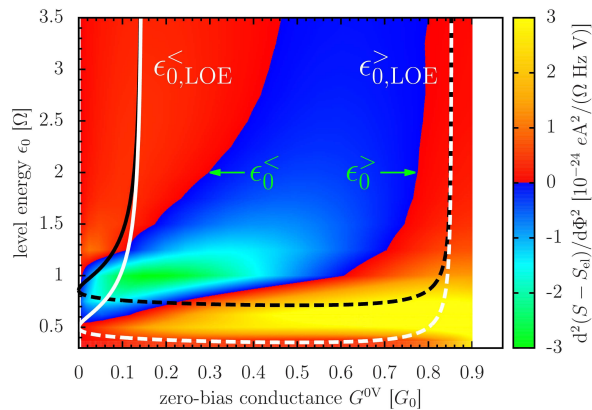


FIG. 4. Inelastic correction to noise at $e\Phi = \Omega$ as a function of zero-bias conductance G^{0V} and energy ϵ_0 of the molecular level. The color map was obtained by a fourth-tier truncation of the HQME approach for $\lambda/\Omega = 0.6$ and $k_B T = 0.0862 \Omega$. For comparison, the solid [dashed] white line shows the transition branch $\epsilon_{0,LOE}^{<}(G^{0V})$ [$\epsilon_{0,LOE}^{>}(G^{0V})$] from positive to negative [negative to positive] inelastic correction obtained on the basis of a LOE in electronic-vibrational coupling, which includes the full energy dependence of the model but treats the vibrational mode in thermal equilibrium [36]. Taking into account the polaron shift, the prediction of the LOE changes to the black lines, $\epsilon_{0,LOE}^{<}>(G^{0V}) \rightarrow \epsilon_{0,LOE}^{<}>(G^{0V}) + \lambda^2/\Omega$.

transition is not constant for $\epsilon_0 > 3\Omega$ yet but still increases which demonstrates that the limit $\epsilon_0 \gg \Omega$ where the extended wide-band approximation applies is not yet reached for $\epsilon_0 = 3.5\Omega$ in the nonequilibrium case. In this limit, perturbative calculations of Novotny *et al.* [39] and Utsumi *et al.* [41] predict the crossovers around a zero-bias conductance of $0.434 G_0$ and $0.816 G_0$. In these studies, the nonequilibrium vibrational distribution function was systematically included in the LOE description by a self-consistent scheme based on the Luttinger-Ward functional [41] or by an infinite resummation of the electron-hole polarization bubble [38, 39, 97].

Next, we investigate how the transitions are influenced by the energy renormalization of the molecular level due to electronic-vibrational coupling, $\epsilon_0 \rightarrow \epsilon_0 - \lambda^2/\Omega$ (polaron shift). This effect is not included in a LOE descrip-

tion. In the limit of vanishing zero-bias conductance, the branch $\epsilon_{0,LOE}^{>}(G^{0V})$ follows the prediction of the LOE for an equilibrated vibration, whereas the branch $\epsilon_{0,LOE}^{<}(G^{0V})$ agrees reasonably well with $\epsilon_{0,LOE}^{<}(G^{0V}) + \lambda^2/\Omega$, which demonstrates that the polaron shift is completely developed in this regime. Consequently, a gap opens for $\epsilon_0 \in [\Omega/2, \Omega]$ where only one transition occurs. The branch $\epsilon_{0,LOE}^{>}(G^{0V})$ increases with rising zero-bias conductance and even crosses $\epsilon_{0,LOE}^{>}(G^{0V}) + \lambda^2/\Omega$ (dashed black line) for $G^{0V} \approx G_0/4$. This behavior might also be attributed to the polaron shift which seems to be fully developed for higher conductance values, whereas it does not play a role for $G^{0V} \rightarrow 0$.

We finally comment on the convergence of the HQME method. A comparison of different hierarchy truncation levels n (data not shown) demonstrates that the HQME results for the conductance and the noise in Fig. 1 are quantitatively converged already for $n = 2$. For the data shown in Figs. 3 and 4, a truncation at $n = 4$ was used. For very large couplings Γ , an even higher truncation would be required to obtain fully quantitative results. This is to be expected because the second derivative of the noise is significantly more difficult to converge than the noise itself or the conductance.

In summary, the HQME method presented here allows the numerically exact evaluation of current fluctuations in nonequilibrium nanosystems with strong electronic-vibrational coupling. The results obtained for a generic model of vibrationally coupled electron transport in molecular junctions demonstrate the importance of cotunneling effects in the nonresonant transport regime and show that the transition from positive to negative inelastic corrections to shot noise depend in a non-universal way on the physical parameters.

While in the present study we have focused on the study of the zero-frequency noise, the method is formulated in a way that it can also describe higher-order current cumulants and the full counting statistics. Furthermore, it can also be applied to models with additional electron-electron interaction [49] and extended to treat explicitly time-dependent problems [98].

We thank A. Erpenbeck, R. Härtle, T. Novotny, and H. Weber for fruitful and inspiring discussions. This work was supported by the German Research Foundation (DFG) via SFB 953 and a research grant.

[1] L. S. Levitov and G. B. Lesovik, Charge distribution in quantum shot noise, *JETP Lett.* **58**, 230 (1993).
 [2] H. Lee, L. S. Levitov, and A. Y. Yakovets, Universal statistics of transport in disordered conductors, *Phys. Rev. B* **51**, 4079 (1995).
 [3] L. S. Levitov, H. Lee, and G. B. Lesovik, Electron counting statistics and coherent states of electric current, *J. Math. Phys.* **37**, 4845 (1996).
 [4] B. Reulet, J. Senzier, and D. E. Prober, Environmental effects in the third moment of voltage fluctuations in a

tunnel junction, *Phys. Rev. Lett.* **91**, 196601 (2003).
 [5] Y. Bomze, G. Gershon, D. Shovkun, L. S. Levitov, and M. Reznikov, Measurement of counting statistics of electron transport in a tunnel junction, *Phys. Rev. Lett.* **95**, 176601 (2005).
 [6] S. Gustavsson, R. Leturcq, B. Simović, R. Schleser, T. Ihn, P. Studerus, K. Ensslin, D. C. Driscoll, and A. C. Gossard, Counting statistics of single electron transport in a quantum dot, *Phys. Rev. Lett.* **96**, 076605 (2006).
 [7] N. Ubbelohde, C. Fricke, C. Flindt, F. Hohls, and R. J.

- Haug, Measurement of finite-frequency current statistics in a single-electron transistor, *Nat. Commun.* **3**, 612 (2012).
- [8] M. J. M. de Jong and C. W. J. Beenakker, Doubled shot noise in disordered normal-metal-superconductor junctions, *Phys. Rev. B* **49**, 16070 (1994).
- [9] X. Jehl, M. Sanquer, R. Calemczuk, and D. Maily, Detection of doubled shot noise in short normal-metal/superconductor junctions, *Nature* **405**, 50 (2000).
- [10] F. Lefloch, C. Hoffmann, M. Sanquer, and D. Quirion, Doubled full shot noise in quantum coherent superconductor-semiconductor junctions, *Phys. Rev. Lett.* **90**, 067002 (2003).
- [11] R. de Picciotto, M. Reznikov, M. Heiblum, V. Umansky, G. Bunin, and D. Mahalu, Direct observation of a fractional charge, *Nature* **389**, 162 (1997).
- [12] L. Saminadayar, D. C. Glattli, Y. Jin, and B. Etienne, Observation of the $e/3$ fractionally charged Laughlin quasiparticle, *Phys. Rev. Lett.* **79**, 2526 (1997).
- [13] H. E. van den Brom and J. M. van Ruitenbeek, Quantum suppression of shot noise in atom-size metallic contacts, *Phys. Rev. Lett.* **82**, 1526 (1999).
- [14] R. Cron, M. F. Goffman, D. Esteve, and C. Urbina, Multiple-charge-quanta shot noise in superconducting atomic contacts, *Phys. Rev. Lett.* **86**, 4104 (2001).
- [15] D. Djukic and J. M. van Ruitenbeek, Shot noise measurements on a single molecule, *Nano Lett.* **6**, 789 (2006).
- [16] M. Kiguchi, O. Tal, S. Wohlthat, F. Pauly, M. Krieger, D. Djukic, J. C. Cuevas, and J. M. van Ruitenbeek, Highly conductive molecular junctions based on direct binding of benzene to platinum electrodes, *Phys. Rev. Lett.* **101**, 046801 (2008).
- [17] O. Tal, M. Krieger, B. Leerink, and J. M. van Ruitenbeek, Electron-vibration interaction in single-molecule junctions: From contact to tunneling regimes, *Phys. Rev. Lett.* **100**, 196804 (2008).
- [18] P. J. Wheeler, J. N. Russom, K. Evans, N. S. King, and D. Natelson, Shot noise suppression at room temperature in atomic-scale Au junctions, *Nano Lett.* **10**, 1287 (2010).
- [19] N. L. Schneider, G. Schull, and R. Berndt, Optical probe of quantum shot-noise reduction at a single-atom contact, *Phys. Rev. Lett.* **105**, 026601 (2010).
- [20] R. Chen, P. J. Wheeler, and D. Natelson, Excess noise in STM-style break junctions at room temperature, *Phys. Rev. B* **85**, 235455 (2012).
- [21] Y. Nazarov and Y. Blanter, *Quantum Transport: Introduction to Nanoscience* (Cambridge University Press, 2009).
- [22] S. Hershfield, J. H. Davies, P. Hyldgaard, C. J. Stanton, and J. W. Wilkins, Zero-frequency current noise for the double-tunnel-junction Coulomb blockade, *Phys. Rev. B* **47**, 1967 (1993).
- [23] A. N. Korotkov, Intrinsic noise of the single-electron transistor, *Phys. Rev. B* **49**, 10381 (1994).
- [24] J. Koch, F. von Oppen, and A. V. Andreev, Theory of the Franck-Condon blockade regime, *Phys. Rev. B* **74**, 205438 (2006).
- [25] F. Haupt, F. Cavaliere, R. Fazio, and M. Sassetti, Anomalous suppression of the shot noise in a nanoelectromechanical system, *Phys. Rev. B* **74**, 205328 (2006).
- [26] C. Flindt, T. c. v. Novotný, A. Braggio, M. Sassetti, and A.-P. Jauho, Counting statistics of non-Markovian quantum stochastic processes, *Phys. Rev. Lett.* **100**, 150601 (2008).
- [27] C. Emary, Counting statistics of tunneling electrons, *Phys. Rev. B* **80**, 235306 (2009).
- [28] M. Esposito and M. Galperin, Self-consistent quantum master equation approach to molecular transport, *J. Phys. Chem. C* **114**, 20362 (2010).
- [29] C. Schinabeck, R. Härtle, H. B. Weber, and M. Thoss, Current noise in single-molecule junctions induced by electronic-vibrational coupling, *Phys. Rev. B* **90**, 075409 (2014).
- [30] K. Kaasbjerg and W. Belzig, Full counting statistics and shot noise of cotunneling in quantum dots and single-molecule transistors, *Phys. Rev. B* **91** (2015).
- [31] B. K. Agarwalla, J.-H. Jiang, and D. Segal, Full counting statistics of vibrationally assisted electronic conduction: Transport and fluctuations of thermoelectric efficiency, *Phys. Rev. B* **92**, 245418 (2015).
- [32] D. S. Kosov, Waiting time distribution for electron transport in a molecular junction with electron-vibration interaction, *J. Chem. Phys.* **146**, 074102 (2017).
- [33] S. L. Rudge and D. S. Kosov, Counting quantum jumps: A summary and comparison of fixed-time and fluctuating-time statistics in electron transport, *J. Chem. Phys.* **151**, 034107 (2019).
- [34] M. Galperin, A. Nitzan, and M. A. Ratner, Inelastic tunneling effects on noise properties of molecular junctions, *Phys. Rev. B* **74**, 075326 (2006).
- [35] H. Haug and A.-P. Jauho, *Quantum Kinetics in Transport and Optics of Semiconductors*, Springer Series in Solid-State Sciences No. Bd. 6 (Springer, 2008).
- [36] R. Avriller and A. Levy Yeyati, Electron-phonon interaction and full counting statistics in molecular junctions, *Phys. Rev. B* **80**, 041309 (2009).
- [37] T. L. Schmidt and A. Komnik, Charge transfer statistics of a molecular quantum dot with a vibrational degree of freedom, *Phys. Rev. B* **80**, 041307 (2009).
- [38] F. Haupt, T. c. v. Novotný, and W. Belzig, Current noise in molecular junctions: Effects of the electron-phonon interaction, *Phys. Rev. B* **82**, 165441 (2010).
- [39] T. c. v. Novotný, F. Haupt, and W. Belzig, Nonequilibrium phonon backaction on the current noise in atom-sized junctions, *Phys. Rev. B* **84**, 113107 (2011).
- [40] T.-H. Park and M. Galperin, Self-consistent full counting statistics of inelastic transport, *Phys. Rev. B* **84**, 205450 (2011).
- [41] Y. Utsumi, O. Entin-Wohlman, A. Ueda, and A. Aharony, Full-counting statistics for molecular junctions: Fluctuation theorem and singularities, *Phys. Rev. B* **87**, 115407 (2013).
- [42] R. Seoane Souto, R. Avriller, R. C. Monreal, A. Martín-Rodero, and A. Levy Yeyati, Transient dynamics and waiting time distribution of molecular junctions in the polaronic regime, *Phys. Rev. B* **92**, 125435 (2015).
- [43] K. Miwa, F. Chen, and M. Galperin, Towards noise simulation in interacting nonequilibrium systems strongly coupled to baths, *Sci. Rep.* **7** (2017).
- [44] B. Dong, G. H. Ding, and X. L. Lei, Full counting statistics of phonon-assisted Andreev tunneling through a quantum dot coupled to normal and superconducting leads, *Phys. Rev. B* **95**, 035409 (2017).
- [45] G. Tang, Y. Xing, and J. Wang, Short-time dynamics of molecular junctions after projective measurement, *Phys. Rev. B* **96**, 075417 (2017).

- [46] P. Stadler, G. Rastelli, and W. Belzig, Finite frequency current noise in the holstein model, *Phys. Rev. B* **97**, 205408 (2018).
- [47] M. Ridley, V. N. Singh, E. Gull, and G. Cohen, Numerically exact full counting statistics of the nonequilibrium anderson impurity model, *Phys. Rev. B* **97**, 115109 (2018).
- [48] R. Härtle, G. Cohen, D. R. Reichman, and A. J. Millis, Decoherence and lead-induced interdot coupling in nonequilibrium electron transport through interacting quantum dots: A hierarchical quantum master equation approach, *Phys. Rev. B* **88**, 235426 (2013).
- [49] R. Härtle, G. Cohen, D. R. Reichman, and A. J. Millis, Transport through an anderson impurity: Current ringing, nonlinear magnetization, and a direct comparison of continuous-time quantum monte carlo and hierarchical quantum master equations, *Phys. Rev. B* **92**, 085430 (2015).
- [50] Y. Tanimura and R. Kubo, Time evolution of a quantum system in contact with a nearly Gaussian-markoffian noise bath, *J. Phys. Soc. Jpn.* **58**, 101 (1989).
- [51] Y. Tanimura, Stochastic liouville, langevin, fokker-planck, and master equation approaches to quantum dissipative systems, *J. Phys. Soc. Jpn.* **75**, 082001 (2006).
- [52] J. Jin, S. Welack, J. Luo, X.-Q. Li, P. Cui, R.-X. Xu, and Y. Yan, Dynamics of quantum dissipation systems interacting with fermion and boson grand canonical bath ensembles: Hierarchical equations of motion approach, *J. Chem. Phys.* **126**, 134113 (2007).
- [53] J. Jin, X. Zheng, and Y. Yan, Exact dynamics of dissipative electronic systems and quantum transport: Hierarchical equations of motion approach, *J. Chem. Phys.* **128**, 234703 (2008).
- [54] X. Zheng, J. Luo, J. Jin, and Y. Yan, Complex non-Markovian effect on time-dependent quantum transport, *J. Chem. Phys.* **130**, 124508 (2009).
- [55] Z. Li, N. Tong, X. Zheng, D. Hou, J. Wei, J. Hu, and Y. Yan, Hierarchical liouville-space approach for accurate and universal characterization of quantum impurity systems, *Phys. Rev. Lett.* **109**, 266403 (2012).
- [56] X. Zheng, Y. Yan, and M. Di Ventra, Kondo memory in driven strongly correlated quantum dots, *Phys. Rev. Lett.* **111**, 086601 (2013).
- [57] Y. Cheng, J. Wei, and Y. Yan, Reappearance of the kondo effect in serially coupled symmetric triple quantum dots, *Europhys. Lett.* **112**, 57001 (2015).
- [58] L. Ye, X. Wang, D. Hou, R.-X. Xu, X. Zheng, and Y. Yan, Heom-quick: a program for accurate, efficient, and universal characterization of strongly correlated quantum impurity systems, *WIREs Comput. Mol. Sci.* **6**, 608 (2016).
- [59] Y. Cheng, Y. Wang, J. Wei, Z. Zhu, and Y. Yan, Long-range exchange interaction in triple quantum dots in the kondo regime, *Phys. Rev. B* **95**, 155417 (2017).
- [60] Z. Li, J. Wei, X. Zheng, Y. Yan, and H.-G. Luo, Corrected kondo temperature beyond the conventional kondo scaling limit, *J. Phys.: Condens. Matter* **29**, 175601 (2017).
- [61] W. Hou, Y. Wang, J. Wei, Z. Zhu, and Y. Yan, Many-body tunneling and nonequilibrium dynamics of doublons in strongly correlated quantum dots, *Sci. Rep.* **7**, 2486 (2017).
- [62] W. Hou, Y. Wang, J. Wei, and Y. Yan, Manipulation of pauli spin blockade in double quantum dot systems, *J. Chem. Phys.* **146**, 224304 (2017).
- [63] R. Härtle and A. J. Millis, Formation of nonequilibrium steady states in interacting double quantum dots: When coherences dominate the charge distribution, *Phys. Rev. B* **90**, 245426 (2014).
- [64] S. Wenderoth, J. Bätge, and R. Härtle, Sharp peaks in the conductance of a double quantum dot and a quantum-dot spin valve at high temperatures: A hierarchical quantum master equation approach, *Phys. Rev. B* **94**, 121303 (2016).
- [65] C. Schinabeck, A. Erpenbeck, R. Härtle, and M. Thoss, Hierarchical quantum master equation approach to electronic-vibrational coupling in nonequilibrium transport through nanosystems, *Phys. Rev. B* **94**, 201407 (2016).
- [66] C. Schinabeck, R. Härtle, and M. Thoss, Hierarchical quantum master equation approach to electronic-vibrational coupling in nonequilibrium transport through nanosystems: Reservoir formulation and application to vibrational instabilities, *Phys. Rev. B* **97**, 235429 (2018).
- [67] C. Flindt, T. Novotný, A. Braggio, and A.-P. Jauho, Counting statistics of transport through coulomb blockade nanostructures: High-order cumulants and non-markovian effects, *Phys. Rev. B* **82**, 155407 (2010).
- [68] S. Wang, X. Zheng, J. Jin, and Y. Yan, Hierarchical liouville-space approach to nonequilibrium dynamical properties of quantum impurity systems, *Phys. Rev. B* **88**, 035129 (2013).
- [69] D. Secker, S. Wagner, S. Ballmann, R. Härtle, M. Thoss, and H. B. Weber, Resonant vibrations, peak broadening, and noise in single molecule contacts: The nature of the first conductance peak, *Phys. Rev. Lett.* **106**, 136807 (2011).
- [70] N. Néel, J. Kröger, and R. Berndt, Two-level conductance fluctuations of a single-molecule junction, *Nano Lett.* **11**, 3593 (2011).
- [71] C. S. Lau, H. Sadeghi, G. Rogers, S. Sangtarash, P. Dallas, K. Porfyrakis, J. Warner, C. J. Lambert, G. A. D. Briggs, and J. A. Mol, Redox-dependent franck-condon blockade and avalanche transport in a graphene-fullerene single-molecule transistor, *Nano Lett.* **16**, 170 (2016).
- [72] E. M. Weig, R. H. Blick, T. Brandes, J. Kirschbaum, W. Wegscheider, M. Bichler, and J. P. Kotthaus, Single-electron-phonon interaction in a suspended quantum dot phonon cavity, *Phys. Rev. Lett.* **92**, 046804 (2004).
- [73] S. Sapmaz, P. Jarillo-Herrero, Y. M. Blanter, C. Dekker, and H. S. J. van der Zant, Tunneling in suspended carbon nanotubes assisted by longitudinal phonons, *Phys. Rev. Lett.* **96**, 026801 (2006).
- [74] R. Leturcq, C. Stampfer, K. Inderbitzin, L. Durrer, C. Hierold, E. Mariani, M. G. Schultz, F. von Oppen, and K. Ensslin, Franck–condon blockade in suspended carbon nanotube quantum dots, *Nat. Phys.* **5**, 327 (2009).
- [75] S. J. van der Molen and P. Liljeroth, Charge transport through molecular switches, *J. Phys.: Condens. Matter* **22**, 133001 (2010).
- [76] J. Gaudioso, L. J. Lauhon, and W. Ho, Vibrationally mediated negative differential resistance in a single molecule, *Phys. Rev. Lett.* **85**, 1918 (2000).
- [77] E. Pop, D. Mann, J. Cao, Q. Wang, K. Goodson, and H. Dai, Negative differential conductance and hot phonons in suspended nanotube molecular wires, *Phys. Rev. Lett.* **95**, 155505 (2005).
- [78] M. Galperin, M. A. Ratner, and A. Nitzan, Hys-

- teresis, switching, and negative differential resistance in molecular junctions: A polaron model, *Nano Lett.* **5**, 125 (2005).
- [79] M. Leijnse and M. R. Wegewijs, Kinetic equations for transport through single-molecule transistors, *Phys. Rev. B* **78**, 235424 (2008).
- [80] R. Härtle and M. Thoss, Resonant electron transport in single-molecule junctions: Vibrational excitation, rectification, negative differential resistance, and local cooling, *Phys. Rev. B* **83**, 115414 (2011).
- [81] J. Koch and F. von Oppen, Franck-Condon blockade and giant Fano factors in transport through single molecules, *Phys. Rev. Lett.* **94**, 206804 (2005).
- [82] R. Härtle, M. Butzin, O. Rubio-Pons, and M. Thoss, Quantum interference and decoherence in single-molecule junctions: How vibrations induce electrical current, *Phys. Rev. Lett.* **107**, 046802 (2011).
- [83] S. Ballmann, R. Härtle, P. B. Coto, M. Elbing, M. Mayor, M. R. Bryce, M. Thoss, and H. B. Weber, Experimental evidence for quantum interference and vibrationally induced decoherence in single-molecule junctions, *Phys. Rev. Lett.* **109**, 056801 (2012).
- [84] J. Koch, M. Semmelhack, F. von Oppen, and A. Nitzan, Current-induced nonequilibrium vibrations in single-molecule devices, *Phys. Rev. B* **73**, 155306 (2006).
- [85] R. Härtle and M. Thoss, Vibrational instabilities in resonant electron transport through single-molecule junctions, *Phys. Rev. B* **83**, 125419 (2011).
- [86] R. Härtle and M. Kulkarni, Effect of broadening in the weak-coupling limit of vibrationally coupled electron transport through molecular junctions and the analogy to quantum dot circuit QED systems, *Phys. Rev. B* **91**, 245429 (2015).
- [87] D. Gelbwaser-Klimovsky, A. Aspuru-Guzik, M. Thoss, and U. Peskin, High-voltage-assisted mechanical stabilization of single-molecule junctions, *Nano Lett.* **18**, 4727 (2018).
- [88] R. Härtle, C. Schinabeck, M. Kulkarni, D. Gelbwaser-Klimovsky, M. Thoss, and U. Peskin, Cooling by heating in nonequilibrium nanosystems, *Phys. Rev. B* **98**, 081404 (2018).
- [89] M. Esposito, U. Harbola, and S. Mukamel, Nonequilibrium fluctuations, fluctuation theorems, and counting statistics in quantum systems, *Rev. Mod. Phys.* **81**, 1665 (2009).
- [90] J. Cerrillo, M. Buser, and T. Brandes, Nonequilibrium quantum transport coefficients and transient dynamics of full counting statistics in the strong-coupling and non-Markovian regimes, *Phys. Rev. B* **94**, 214308 (2016).
- [91] J. Jin, S. Wang, X. Zheng, and Y. Yan, Current noise spectra and mechanisms with dissipative equation of motion theory, *J. Chem. Phys.* **142**, 234108 (2015).
- [92] J. Koch, M. E. Raikh, and F. von Oppen, Full counting statistics of strongly non-ohmic transport through single molecules, *Phys. Rev. Lett.* **95**, 056801 (2005).
- [93] V. N. Golovach and D. Loss, Transport through a double quantum dot in the sequential tunneling and cotunneling regimes, *Phys. Rev. B* **69**, 245327 (2004).
- [94] N. M. Gergs, C. B. M. Horig, M. R. Wegewijs, and D. Schuricht, Charge fluctuations in nonlinear heat transport, *Phys. Rev. B* **91**, 201107 (2015).
- [95] M. Kumar, R. Avriller, A. L. Yeyati, and J. M. van Ruitenbeek, Detection of vibration-mode scattering in electronic shot noise, *Phys. Rev. Lett.* **108**, 146602 (2012).
- [96] R. Avriller and T. Frederiksen, Inelastic shot noise characteristics of nanoscale junctions from first principles, *Phys. Rev. B* **86**, 155411 (2012).
- [97] J. K. Viljas, J. C. Cuevas, F. Pauly, and M. Häfner, Electron-vibration interaction in transport through atomic gold wires, *Phys. Rev. B* **72**, 245415 (2005).
- [98] M. Benito, M. Niklas, and S. Kohler, Full-counting statistics of time-dependent conductors, *Phys. Rev. B* **94**, 195433 (2016).